Available online at www.sciencedirect.com
ScienceDirect
Biochemical and Biophysical Research Communications 368 (2008) 74–80
BBRC
www.elsevier.com/locate/ybbrc

Phage display based identification of novel stabilizing mutations in glycosyl hydrolase family 11 *B. subtilis* endoxylanase XynA

Tim Beliën *, Priscilla Verjans, Christophe M. Courtin, Jan A. Delcour

Faculty of Applied Bioscience and Engineering, Laboratory of Food Chemistry and Biochemistry, Katholieke Universiteit Leuven, Kasteelpark Arenberg 20, B-3001 Leuven, Belgium

Received 4 January 2008
Available online 28 January 2008

Abstract

Two combinatorial libraries of glycosyl hydrolase family 11 (GH11) *Bacillus subtilis* endoxylanase XynA were constructed and displayed on phage. Both phage-displayed libraries were subjected to three consecutive biopanning rounds against immobilized endoxylanase inhibitor TAXI, each time preceded by an incubation step at elevated temperature. DNA sequence analysis of enriched phagemid panning isolates allowed identification of mutations conferring enhanced thermal stability. In particular, substitutions T44C, T44Y, F48C, T87D, and Y94C were retained, and their thermostabilizing effect was confirmed by testing site-directed XynA variants. None of these mutations was identified in earlier endoxylanase engineering studies. Each single mutation increased the half-inactivation temperature by 2–3 °C over that of the wild-type enzyme. Intriguingly, the three selected cysteine variants generated dimers by formation of intermolecular disulfide bridges.

Keywords: Endoxylanase; Molecular evolution; Phage display; Thermostability

Endo-β-1,4-xylanases (EC 3.2.1.8) (further referred to as endoxylanases) are crucial for (arabino)xylan depolymerisation, as they break down the xylan backbone by catalyzing the hydrolysis of β-1,4-xylan linkages. Their substrate is the predominant hemicellulose in cell walls of plants and the second most abundant polysaccharide on earth. Endoxylanases are widely used as improvers and processing aids in biotechnological processes such as industrial bread-making, feed production, biobleaching of pulps in paper manufacturing, and bioconversion of agricultural residues to fuel ethanol [1]. Apart from this, endoxylanases of microbial origin play an important role in phytopathogenesis, as they provide essential means to attacking microorganisms to break through the plant cell wall [2]. Based on amino acid sequence similarities and hydrophobic cluster analysis, endoxylanases have been classified mainly into glycosyl hydrolase families (GH) 10 and 11 [3]. GH11 endoxylanases adopt a β-jelly-roll fold, in which two large β-pleated sheets and one α-helix form a structure that resembles a partly-closed right hand [4].

An important factor governing endoxylanase functionality in industrial applications is their stability under the often harsh conditions of biotechnological processes. Many endoxylanases used in industry today are of mesophilic origin. As a consequence, numerous protein engineering efforts have been directed towards improvement of their thermostability. Among them, many studies focussed on the designed incorporation of intramolecular disulfide bridges [5–12]. Other rational design approaches include the introduction of surface charges [13,14], aromatic interactions [15] or a thermostabilizing N-terminal domain [16]. In addition, several directed evolution tactics were applied, in which the endoxylanase encoding gene was subjected to random mutagenesis over its full length [17–21].

We here report on the identification of thermostabilizing mutations in the *B. subtilis* GH11 endoxylanase by use of a newly developed phage display based selection system. In

* Corresponding author. Fax: +32 16 321997.
E-mail address: tim.belien@biw.kuleuven.be (T. Beliën).

0006-291X/$ - see front matter © 2008 Elsevier Inc. All rights reserved.
doi:10.1016/j.bbrc.2008.01.047

contrast to previous studies, our method involved a semi-rational molecular evolution approach, since variation was introduced in a controlled way and was restricted to delineated regions of the enzyme.

Materials and methods

Strains, plasmids, phagemid, and helper phage. *Escherichia coli* CJ236 (FΔ(HindIII)*::cat* (Tra$^+$ Pil$^+$ Cm^r)/*ung*$^{-1}$ *relA1 dut*$^{-1}$ *thi*$^{-1}$ *spoT1 mcrA*) (New England Biolabs) and helper phage R408 (Stratagene) were used for preparation of deoxy-uridine-containing single stranded (dU-ss)DNA. *E. coli* TG1 (*supE hsdΔ5 thi Δ*(*lac-proAB*) F′ [*traD36 proAB*$^+$ *lacI*^{q} *lacZΔM15*]) was used for transformation of the phagemid pHOS31 library and as acceptor strain for helper phage VCSM13 (Stratagene) and phage infections during successive rounds of biopanning. *E. coli* XL1-Blue MRF′ (*supE44 hsdR17 recA1 endA1 gyrA46 thi relA1 lac*$^-$ *Δ*(*mcrA*)*183 Δ*(*mcrCB-hsdSMR-mrr*)*173* F′ [*proAB*$^+$ *lacI*^{q} *lacZΔM15* Tn*10* (*tet*^{r})]) (Stratagene) and *E. coli* BL21 (DE3) (F$^-$ *dcm ompT hsdS* (r_B^- m_B^-) *gal* (*DE3*)) were used as host strain for subcloning and heterologous expression via expression vector pEXP5-CT (Invitrogen), respectively.

Construction of the xynA combinatorial libraries. The phage-displayed combinatorial *xynA* libraries were constructed essentially as described earlier [22]. Briefly, pHOS31-*xynA* dU-ss-DNA was used as template for the Kunkel mutagenesis method with either mutagenic oligonucleotide LibG39-F48 or LibT87-K95 (Table 1) designed to introduce mutations at the regions connecting β-strands B3 and A5, and B6 and B9, respectively. *E. coli* TG1 electrocompetent cells were transformed with each mutagenesis reaction mixture and after coinfection with VCSM13 phages were produced during overnight incubation at 37 °C. Phage particles were precipitated as described elsewhere [22] and resuspended in phosphate buffered saline (PBS). Prior to selection, phage solutions were cleared from traces of polyethylene glycol (PEG) by centrifugation through Microcon YM-100 filters (Millipore).

Selection and enrichment of the xynA combinatorial libraries. To select for stabilizing mutations, the biopanning rounds were preceded by an extra incubation step under denaturing conditions. Phage preparations (~4×10^{10} colony forming units, CFU) were heated to 60 °C for 15 min. After cooling to room temperature, phage solutions were added to Maxisorb™ plate (Nalge Nunc International) wells, which were coated with ~1 μg endoxylanase inhibitor TAXI. Following a 2-h incubation to allow phage binding, the plates were washed eight times with PBS and eight times with PBS containing 0.1% Tween-20. Bound phages were eluted by 10 min incubation with 100 mM triethyl amine (pH 12.0) and the eluate was neutralized with 1.0 M Tris–HCl, pH 7.4. For all selections, an equal number of uncoated wells were used as negative control. A fraction (~1/100 volume) of the neutralized eluted phage solution was plated in serial dilutions on selective agar plates (containing 100 μg/ml ampicillin) to determine the phage titers. Eluted phages were amplified in *E. coli* TG1 and used for further rounds of selection. The selection process was monitored by titering the phage suspensions before selection and after elution.

DNA sequencing. Phagemid and expression plasmid inserts were sequenced by the chain-termination dideoxynucleoside triphosphate method with the BigDye® Terminator V3.1 CycleSequencing Kit (Applied Biosystems) and vector-specific primers.

Site-directed mutagenesis and recombinant expression. Expression plasmid pEXP5-CT-*xynA* was constructed for use as vector for heterologous expression in *E. coli*. To this end, *xynA* was PCR amplified with primer couple XynApEXf/XynATOPOr (Table 1) using pQE-EN-*xynA* [23] as template. The resulting PCR product was cloned into the pEXP5-CT/TOPO vector (Invitrogen). Site-directed mutagenesis was carried out using the Quick Change Site-Directed Mutagenesis Kit (Stratagene) with pEXP5-CT-*xynA* as template DNA and a pair of complementary mutagenic primers according to the manufacturer's instructions. Table 1 lists sequences of the forward primers for each mutation.

Recombinant XynA and variants thereof were produced in *E. coli* BL21 (DE3) cells transformed with pEXP5-CT-*xynA* or mutant constructs, respectively. Protein expression was performed according to instructions of the pEXP5-CT/TOPO TA Expression Kit (Invitrogen). Cultures were grown in tryptone and yeast extract medium (2× TY) supplemented with 100 μg/ml ampicillin at 37 °C with shaking at 250 rpm until the absorbance at 600 nm (A_{600}) reached approximately 0.5. Expression was induced with isopropyl-β-D-thiogalactopyranoside (IPTG) (0.2 mM) and cells were further grown at 18 °C. After ~18 h incubation, cells were harvested by centrifugation at 2800*g* for 20 min. Pellets were resuspended in an appropriate amount of lysis buffer (20 mM NaH_2PO_4, 500 mM NaCl, 30 mM imidazole, pH 7.4) for a 50-fold concentration of cell density. Protease inhibitor Pefablock® SC (Merck-Eurolab) was added to a final concentration of 1 mM. Lysis was performed by incubation with 1.0 mg/ml lysozyme (Sigma–Aldrich) for 30 min on ice followed by three cycles of freeze-thawing (−80 °C to 25 °C) and sonication on ice (three bursts of 15 s with 1 min pause in between for 2.0 ml lysates by using the microtip of a Vibra Cell™ model VCX 13 PB sonicator (Sonics & Materials) set at an amplitude of 40%). Ni–NTA Spin Columns (Qiagen) were used to purify the His_6-tagged proteins from the lysate under native conditions according to the manufacturer's instructions. Protein expression and purification were assessed by standard sodium dodecyl sulfate–polyacrylamide gel electrophoresis (SDS–PAGE) and Coomassie blue staining. Protein concentrations were estimated after digitalization of gels with Un-Scan-it gel version 5.1 software (Silk Scientific). The low molecular weight SDS–PAGE marker of Amersham Biosciences was used to compare band sizes.

Endoxylanase activity and functional stability assay. Enzyme activity of recombinant endoxylanase was determined with the colorimetric Xylazyme-AX method (Megazyme). Ni–NTA purified endoxylanase fractions were diluted in 0.5 ml sodium acetate buffer (25 mM, pH 5.5). The

Table 1
Oligonucleotides used in this study

	Sequence	Mutated residue(s)
XynApEXf	5′-ATGGCTAGCACAGATTACTGGCAAAATTG	
XynATOPOr	5′-CCACACTGTTACATTAGAAC	
LibG39-F48r	5′-CGGCGCCCAAACTCCGGCATTATAGTTTATCGTCC TA**AHRCSRCNM**ACC**GNHAVH**CCAACC**MNHACV**AACAACAAAATTTCCGGTATTAGACC	G^{39}–K^{40}–T^{43}–T^{44}–S^{46}– P^{47}–F^{48}
LibT87-K95r	5′-GTCATATGTACCCCCATCACTTTTTACAGTACC**MN** **WANNGDH**TCC**ADW**AGG**TYY**ATA**MBH**ACCCCATGAATCCACTACATAATATTCTATGAGAGG	T^{87}–R^{89}–T^{91}–Y^{93}–Y^{94}– K^{95}
XynA-T44Cf	5′-GTTGTTGGTAAAGGTTGGACT**TGC**GGTTCGCCATTTAGGACG	$T^{44} \rightarrow C^{44}$
XynII-T44Yf	5′-GTTGTTGGTAAAGGTTGGACT**TAC**GGTTCGCCATTTAGGACG	$T^{44} \rightarrow Y^{44}$
XynA-F48Cf	5′-GGACTACAGGTTCGCCA**TGT**AGGACGATAAACTATAATG	$F^{48} \rightarrow C^{48}$
XynA-T87Df	5′-GTAGTGGATTCATGGGGT**GAT**TATAGACCTACTGGAACG	$T^{87} \rightarrow D^{87}$
XynA-Y94Cf	5′-GACCTACTGGAACG**TGT**AAAGGTACTGTAAAAAGTG	$Y^{94} \rightarrow C^{94}$

Underlined nucleotides correspond to mutated codons, bold nucleotides correspond to mutations, degeneracies are indicated as follows: H, A/C/T; R, A/G; S, G/C; N, A/C/G/T; M, A/C; V, A/C/G; W, A/T; D, A/G/T; Y, C/T; B, C/G/T.

suspension was incubated for 10 min at 40 °C, prior to addition of a Xylazyme AX tablet. These tablets consist of azurine-crosslinked wheat arabinoxylan, which, upon hydrolysis by endoxylanase, produces water-soluble dyed fragments, the rate of release of which (increase of A_{590}) can be related directly to enzyme activity. Incubation was prolonged for 60 min at 40 °C and stopped by adding 2.0% (w/v) Trizma base solution (5.0 ml) and vortex stirring. After filtering through a 90 mm filter (Merck-Eurolab), the A_{590} of filtrates was measured. One enzyme unit (EU) corresponds to an increase in A_{590} of 1.0 under the conditions of the assay. Functional temperature stability of recombinant XynA and mutants was determined by incubating the enzymes (~1 μg/ml) at various temperatures (from 45 to 65 °C) for 10 min. After cooling the samples in an ice water bath, residual activities were determined at 40 °C. All tests were performed in triplicate and data were analyzed by non-linear regression fits using GraphPad Prism software. Good correlations were obtained for all fits ($R^2 > 0.99$).

Results and discussion

High-throughput selection strategy for enhanced thermostability

The functional display of endoxylanases on phage particles [23] opens perspectives to study, improve or alter their biochemical properties using displayed combinatorial protein libraries. Screening of such libraries allows for the exhaustive exploration of a defined region of sequence space within the protein [24]. For instance, following binding selection and sequence analysis of endoxylanase displaying phages, the contribution of several residues to inhibitor interaction could be deduced based on obtained amino acid frequencies, since these correlated well with the functional importance for the selected feature [22,25]. Here, we extended the previously developed phage display based endoxylanase selection system to screen for thermostabilizing mutations. In adapting phage display technology from the more common selection for binding affinity, displayed proteins undergo an extra selection step by incubating recombinant phage particles under denaturing conditions prior to their capture on immobilized ligands [26,27]. Since only variants that retain binding capacity are captured, stabilizing mutations are enriched during consecutive panning rounds, with the implicit assumption that a properly folded protein is required for an intact binding interface.

In this study, two combinatorial libraries of the GH11 *B. subtilis* endoxylanase XynA were constructed and displayed on phage. Combinatorial variety was restricted to the region connecting β-strands B3 and A5 on the one hand (Fig. 1A), and the region connecting β-strands B6 and B9

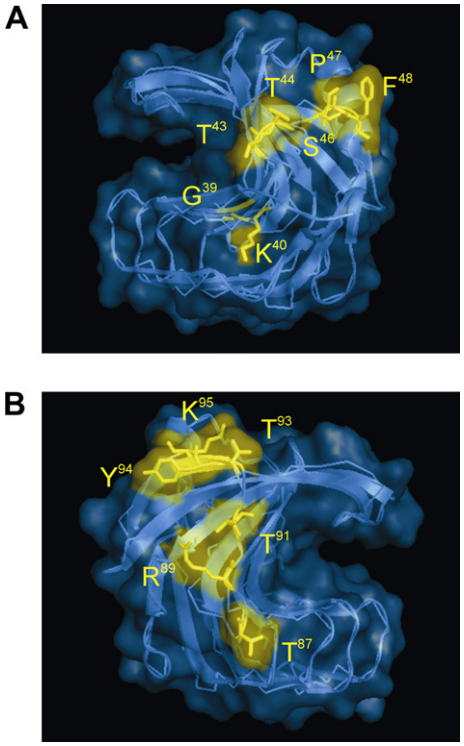

Fig. 1. Molecular view of the XynA protein (PDB code 1XNN), showing the location of the amino acids targeted for mutagenesis. (A) Residues of the first combinatorial library (region connecting β-strands B3 and A5) are highlighted. (B) Residues of the second combinatorial library (region connecting β-strands B6 and B9) are highlighted. Both figures were generated using Pymol (http://pymol.sourceforge.net/).

Table 2
Enrichment of XynA mutant phages from both combinatorial libraries selected against TAXI during three consecutive panning rounds

	Library/ selection temperature	Titer of eluted phages (CFU/ml)	Recovery (output/ input)[a]	Enrichment ratio[b]
LibG39-F48/40 °C				
Uncoated	Round 1	$<1 \times 10^4$	$<2.5 \times 10^{-7}$	
wells (BSA)	Round 2	$<1 \times 10^4$	$<2.5 \times 10^{-7}$	
	Round 3	$\sim 1 \times 10^4$	2.5×10^{-7}	
Wells coated	Round 1	$\sim 4 \times 10^6$	1×10^{-4}	>400
with TAXI	Round 2	$\sim 2 \times 10^7$	5×10^{-4}	>2000
	Round 3	$\sim 4 \times 10^7$	1×10^{-5}	4000
LibG39-F48 / 60 °C				
Uncoated	Round 1	$<1 \times 10^4$	$<2.5 \times 10^{-7}$	
wells (BSA)	Round 2	$<1 \times 10^4$	$<2.5 \times 10^{-7}$	
	Round 3	$\sim 2 \times 10^4$	5×10^{-7}	
Wells coated	Round 1	$\sim 5 \times 10^4$	1.25×10^{-6}	>5
with TAXI	Round 2	$\sim 2 \times 10^6$	5×10^{-5}	>200
	Round 3	$\sim 1 \times 10^7$	2.5×10^{-4}	500
LibT87-K95/40 °C				
Uncoated	Round 1	$<1 \times 10^4$	$<2.5 \times 10^{-7}$	
wells (BSA)	Round 2	$<1 \times 10^4$	$<2.5 \times 10^{-7}$	
	Round 3	$\sim 1 \times 10^4$	2.5×10^{-7}	
Wells coated	Round 1	$\sim 2 \times 10^6$	5×10^{-5}	>200
with TAXI	Round 2	$\sim 1 \times 10^7$	2.5×10^{-4}	>1000
	Round 3	$\sim 3 \times 10^7$	7.5×10^{-4}	3000
LibT87-K95/60 °C				
Uncoated	Round 1	$<1 \times 10^4$	$<2.5 \times 10^{-7}$	
wells (BSA)	Round 2	$<1 \times 10^4$	$<2.5 \times 10^{-7}$	
	Round 3	$\sim 3 \times 10^4$	7.5×10^{-7}	
Wells coated	Round 1	$\sim 4 \times 10^4$	1×10^{-6}	>4
with TAXI	Round 2	$\sim 3 \times 10^6$	7.5×10^{-5}	>300
	Round 3	$\sim 4 \times 10^7$	1×10^{-3}	1333

[a] Recovery of the indicated selection round was estimated by dividing the number of eluted phages by the number of phages applied to the well ($\sim 4 \times 10^{10}$ CFU).

[b] The titer of phages eluted from wells coated with target protein divided by the titer of phages eluted from uncoated wells.

on the other (Fig. 1B). These regions were targeted, firstly because they are located outside the active cleft (but instead on opposite sides of it, Fig. 1), and hence, do not directly affect the catalytic activity, secondly, because in neither of both regions stabilizing substitutions could be detected by previous directed evolution approaches [17–21]. The generated diversity was not totally at random as residues displaying unfavorable torsion angles at the distinct positions (as indicated by structural analysis using Pymol software, Delano Scientific) were underrepresented in the designed degenerated codons, wherever possible, taking into account the nature of the genetic code (Table 1). Hence, the restricted set of substitutions introduced in the libraries was expected to enhance the likelihood of identifying stabilizing mutations. Moreover, by choosing a limited number of substitutions at defined positions, in contrast to complete randomization, diverse yet manageable populations of molecules were obtained. The libraries generated after several transformations contained $\sim 3 \times 10^8$ unique members, and DNA sequencing of several randomly picked clones of each naive library revealed that roughly 50% of them had incorporated the mutagenic

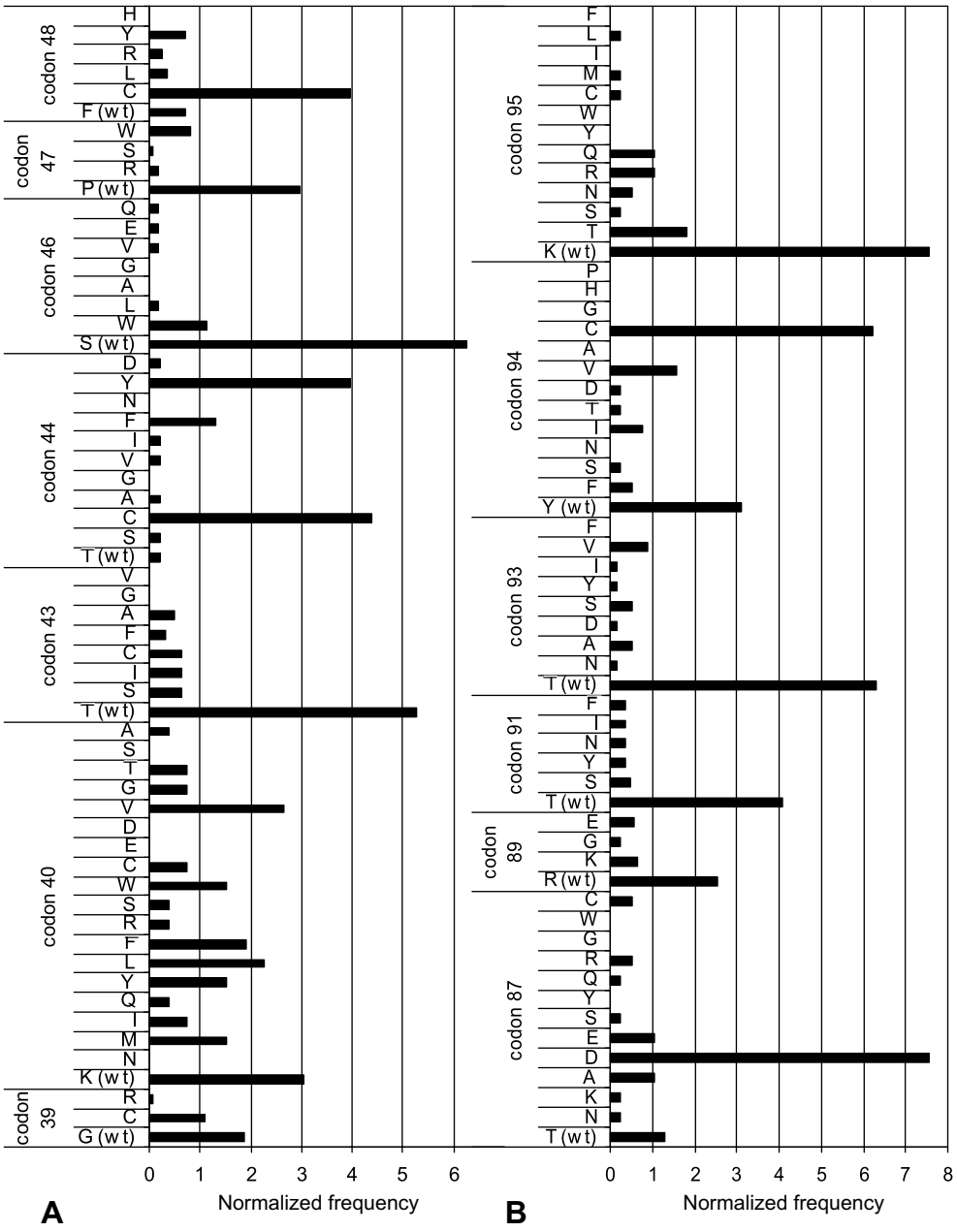

Fig. 2. Mutant amino acid frequencies of occurrence in the enriched GH11 endoxylanase combinatorial libraries comprising β-strands B3 and A5 (A), and β-strands B6 and B9 (B). For each mutated position the following procedure [22] was applied: counted number of each encoded amino acid/total number of sequenced clones (50) × # different amino acids encoded in the library at that position.

oligonucleotide. Hence, the theoretical diversity for combinatorial mutagenesis at the selected positions ($\sim 1.5 \times 10^6$ and $\sim 9.9 \times 10^5$, respectively) was exceeded by at least 10^2-fold.

Biopanning and sequence analysis of the phage-displayed combinatorial libraries

Both phage-displayed libraries were subjected to three consecutive biopanning rounds against immobilized TAXI, each time preceded by incubation at control (40 °C) and elevated temperature (60 °C). Table 2 shows that the titer of phages pre-incubated at 40 °C after the first round was already considerably higher for selection against TAXI than for selection in control wells [uncoated wells blocked with bovine serum albumin (BSA)]. This initial strong enrichment increased only slightly (~2–5-fold) throughout the panning procedure, reflecting the fact that no selection pressure was exerted on the phage pools. In contrast, the enrichment ratio of phages pre-incubated at 60 °C enlarged up to ~100-fold after a panning round against TAXI (Table 2). These data clearly pointed to functional selection of thermostabilized endoxylanase variants.

After three rounds of biopanning, the XynA sequence of 50 clones of each enriched library was sequenced. At each mutated position, the occurrences of wild-type or each targeted substitution were tabulated. Their percentage contribution was calculated and normalized to the total number of different amino acids encoded in the library at that position, as described previously [22] (Fig. 2). The obtained frequency of occurrence of specific amino acids at the mutated positions indicates the importance of these residues for adaptation to the selection pressure, and, hence, the stabilization of the enzyme. Fig. 2 shows that wild-type residues were, in general, quite well represented in the enriched phage pools. Still, based on the most striking frequencies, one can deduce that the following mutations had a stabilizing effect: T44C, T44Y, F48C, T87D, and Y94C.

Evaluation of functional temperature stability of enriched XynA mutants

The impact of mutations T44C, T44Y, F48C, T87D, and Y94C on enzyme thermostabilization as deduced from the screening results was verified by construction of site directed mutants of each of them. After recombinant expression in *E. coli* via expression vector pEXP5-CT and subsequent Ni–NTA purification, their functional temperature stability was measured. All five mutants displayed an improved thermostability in comparison to the wild-type enzyme (Fig. 3). The half-inactivation temperatures (midpoints of the inactivation curves) of the mutants increased with ~3 (±0.15) °C and ~2 (±0.15) °C for F48C/Y94C and T44Y/T44C/T87D, respectively. While the wild-type enzyme completely lost activity after pre-incubation at 60 °C, the mutants retained 5–10% of their activity under the conditions of the assay.

Since three enriched mutations involved the introduction of a cysteine residue at the surface of the enzyme, we wondered whether potential dimer formation occurred

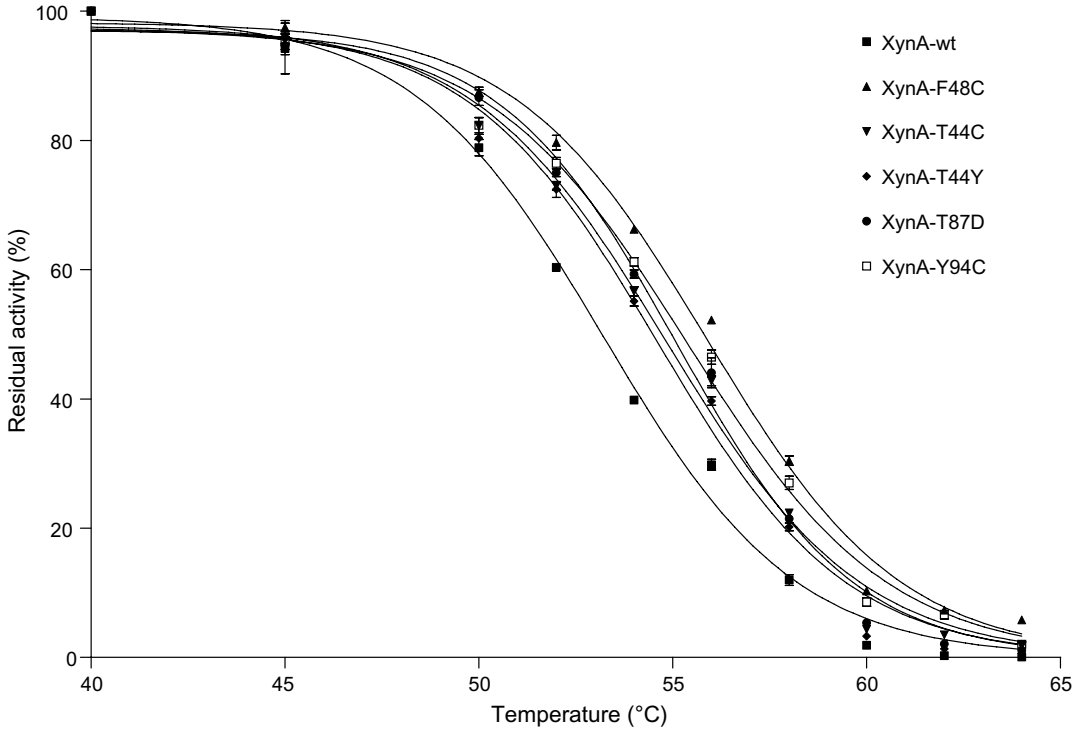

Fig. 3. Functional temperature stability of wild-type XynA and selected mutants. Residual activities are relative to the activities measured after heat treatment at 40 °C for 10 min, which were expressed as 100%. Means and standard deviations of triplicate experiments are shown.

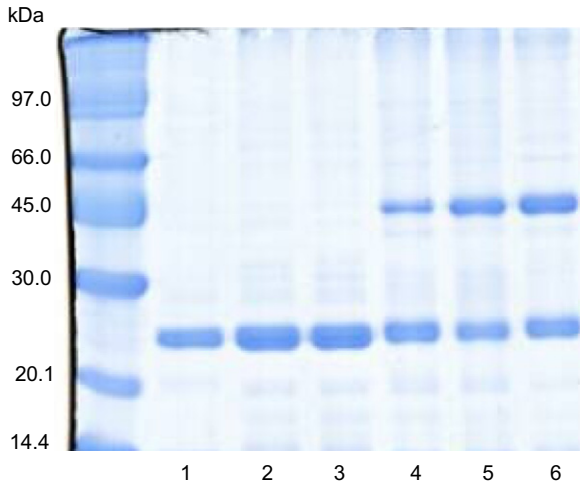

Fig. 4. SDS–PAGE analysis of purified Cys mutants. Samples were incubated in presence and absence of DTT (1 mM). Lane 1, low molecular weight protein marker; lane 2, XynA-Y94C (+DTT); lane 3, XynA-T44C (+DTT); lane 4, XynA-F48C (+DTT); lane 5, XynA-Y94C (−DTT); lane 6, XynA-T44C (−DTT); lane 7, XynA-F48C (−DTT).

through intermolecular disulfide bridges. To check this possibility, XynA-T44C, XynA-F48C, and XynA-Y94C were incubated both in presence and absence of the reducing agent dithioreitol (DTT, 1 mM) and subjected to SDS–PAGE. Fig. 4 shows that, in presence of DTT, the purified enzymes migrated as single bands with apparent molecular weights of ~23 kDa, which is in good agreement with the molecular mass of the native His-tagged monomer. In absence of DTT, however, all three Cys mutants migrated partly as dimers with an apparent molecular mass of ~45 kDa, revealing the formation of intermolecular disulfide bridges. Presumably, dimerization of the Cys mutants also occurred on the surface of phage particles during the selection process. Protein dimerization can indeed take place in phage display formats as has been repeatedly shown in previous studies [28–30]. Although GH11 endoxylanases have been extensively subjected to protein engineering approaches to improve their stability, formation of intermolecular disulfide bridges—in contrast to intramolecular disulfide bridges [5–12]—has been achieved very rarely. In fact, to the best of our knowledge, only substitution of Ser at position 179 by Cys has been reported [20] to give rise to a disulfide linked dimer. However, even for this endoxylanase variant there is no consensus on intermolecular disulfide bridge formation, as different forms (dimeric or monomeric) are observed by different authors [5,20,21]. In addition, the enlargement of hydrophobic contact between monomers, rather than disulfide bridge linking, has been suggested to account for the thermostabilizing effect of the S179C mutation [20]. The same probably applies for the T44C mutation identified here, as replacement of Thr^{44} by the hydrophobic side chain of Tyr resulted in a variant with similar stability. Mutants XynA-F48C and XynA-Y94C, on the other hand, seem to be stabilized exclusively through formation of the intermolecular disulfide bridge. Variant XynA-T87D, finally, is most likely stabilized by creation of an additional salt-bridge between Asp^{87} and Lys^{135} as the carboxyl group of the former is modeled to be in close proximity (~4 Å) to the positively charged ammonium group of the latter.

Acknowledgment

The authors wish to thank financial support (post-doctoral research fellowship of T. Beliën) by the Flemish IWT (*Instituut voor de aanmoediging van Innovatie door Wetenschap en Technologie in Vlaanderen*).

References

[1] M.L. Polizeli, A.C. Rizzatti, R. Monti, H.F. Terenzi, J.A. Jorge, D.S. Amorim, Xylanases from fungi: properties and industrial applications, Appl. Microbiol. Biotechnol. 67 (2005) 577–591.
[2] T. Belien, S. Van Campenhout, J. Robben, G. Volckaert, Microbial endoxylanases: effective weapons to breach the plant cell-wall barrier or, rather, triggers of plant defense systems? Mol. Plant Microbe Interact. 19 (2006) 1072–1081.
[3] B. Henrissat, A classification of glycosyl hydrolases based on amino acid sequence similarities, Biochem. J. 280 (Pt 2) (1991) 309–316.
[4] A. Torronen, J. Rouvinen, Structural and functional properties of low molecular weight endo-1,4-beta-xylanases, J. Biotechnol. 57 (1997) 137–149.
[5] W.W. Wakarchuk, W.L. Sung, R.L. Campbell, A. Cunningham, D.C. Watson, M. Yaguchi, Thermostabilization of the *Bacillus circulans* xylanase by the introduction of disulfide bonds, Protein Eng. 7 (1994) 1379–1386.
[6] O. Turunen, K. Etuaho, F. Fenel, J. Vehmaanpera, X. Wu, J. Rouvinen, M. Leisola, A combination of weakly stabilizing mutations with a disulfide bridge in the alpha-helix region of *Trichoderma reesei* endo-1,4-beta-xylanase II increases the thermal stability through synergism, J. Biotechnol. 88 (2001) 37–46.
[7] F. Fenel, M. Leisola, J. Janis, O. Turunen, A de novo designed N-terminal disulphide bridge stabilizes the *Trichoderma reesei* endo-1,4-beta-xylanase II, J. Biotechnol. 108 (2004) 137–143.
[8] H. Xiong, F. Fenel, M. Leisola, O. Turunen, Engineering the thermostability of *Trichoderma reesei* endo-1,4-beta-xylanase II by combination of disulphide bridges, Extremophiles 8 (2004) 393–400.
[9] G. Paes, M.J. O'Donohue, Engineering increased thermostability in the thermostable GH-11 xylanase from *Thermobacillus xylanilyticus*, J. Biotechnol. 125 (2006) 338–350.
[10] J. Davoodi, W.W. Wakarchuk, P.R. Carey, W.K. Surewicz, Mechanism of stabilization of *Bacillus circulans* xylanase upon the introduction of disulfide bonds, Biophys. Chem. 125 (2007) 453–461.
[11] M.Y. Jeong, S. Kim, C.W. Yun, Y.J. Choi, S.G. Cho, Engineering a de novo internal disulfide bridge to improve the thermal stability of xylanase from *Bacillus stearothermophilus* No. 236, J. Biotechnol. 127 (2007) 300–309.
[12] H.M. Yang, B. Yao, K. Meng, Y.R. Wang, Y.G. Bai, N.F. Wu, Introduction of a disulfide bridge enhances the thermostability of a *Streptomyces olivaceoviridis* xylanase mutant, J. Ind. Microbiol. Biotechnol. 34 (2007) 213–218.
[13] O. Turunen, M. Vuorio, F. Fenel, M. Leisola, Engineering of multiple arginines into the Ser/Thr surface of *Trichoderma reesei* endo-1,4-beta-xylanase II increases the thermotolerance and shifts the pH optimum towards alkaline pH, Protein Eng. 15 (2002) 141–145.
[14] R. Sriprang, K. Asano, J. Gobsuk, S. Tanapongpipat, V. Champreda, L. Eurwilaichitr, Improvement of thermostability of fungal xylanase by using site-directed mutagenesis, J. Biotechnol. 126 (2006) 454–462.
[15] J. Georis, F. de Lemos Esteves, J. Lamotte-Brasseur, V. Bougnet, B. Devreese, F. Giannotta, B. Granier, J.M. Frere, An additional

aromatic interaction improves the thermostability and thermophilicity of a mesophilic family 11 xylanase: structural basis and molecular study, Protein Sci. 9 (2000) 466–475.
[16] J.Y. Sun, M.Q. Liu, Y.L. Xu, Z.R. Xu, L. Pan, H. Gao, Improvement of the thermostability and catalytic activity of a mesophilic family 11 xylanase by N-terminus replacement, Protein Expr. Purif. 42 (2005) 122–130.
[17] A. Arase, T. Yomo, I. Urabe, Y. Hata, Y. Katsube, H. Okada, Stabilization of xylanase by random mutagenesis, FEBS Lett. 316 (1993) 123–127.
[18] N. Palackal, Y. Brennan, W.N. Callen, P. Dupree, G. Frey, F. Goubet, G.P. Hazlewood, S. Healey, Y.E. Kang, K.A. Kretz, E. Lee, X. Tan, G.L. Tomlinson, J. Verruto, V.W. Wong, E.J. Mathur, J.M. Short, D.E. Robertson, B.A. Steer, An evolutionary route to xylanase process fitness, Protein Sci. 13 (2004) 494–503.
[19] D.E. Stephens, K. Rumbold, K. Permaul, B.A. Prior, S. Singh, Directed evolution of the thermostable xylanase from *Thermomyces lanuginosus*, J. Biotechnol. 127 (2007) 348–354.
[20] K. Miyazaki, M. Takenouchi, H. Kondo, N. Noro, M. Suzuki, S. Tsuda, Thermal stabilization of *Bacillus subtilis* family-11 xylanase by directed evolution, J. Biol. Chem. 281 (2006) 10236–10242.
[21] R. Ruller, L. Deliberto, T.L. Ferreira, R.J. Ward, Thermostable variants of the recombinant xylanase a from *Bacillus subtilis* produced by directed evolution show reduced heat capacity changes, Proteins (2007).
[22] T. Belien, S. Van Campenhout, A.V. Bosch, T.M. Bourgois, S. Rombouts, J. Robben, C.M. Courtin, J.A. Delcour, G. Volckaert, Engineering molecular recognition of endoxylanase enzymes and their inhibitors through phage display, J. Mol. Recognit. 20 (2007) 103–112.
[23] T. Belien, K. Hertveldt, K. Van den Brande, J. Robben, S. Van Campenhout, G. Volckaert, Functional display of family 11 endoxylanases on the surface of phage M13, J. Biotechnol. 115 (2005) 249–260.
[24] J. Pelletier, S. Sidhu, Mapping protein–protein interactions with combinatorial biology methods, Curr. Opin. Biotechnol. 12 (2001) 340–347.
[25] T. Belien, S. Van Campenhout, M. Van Acker, J. Robben, C.M. Courtin, J.A. Delcour, G. Volckaert, Mutational analysis of endoxylanases XylA and XylB from the phytopathogen *Fusarium graminearum* reveals comprehensive insights into their inhibitor insensitivity, Appl. Environ. Microbiol. 73 (2007) 4602–4608.
[26] S. Jung, A. Honegger, A. Pluckthun, Selection for improved protein stability by phage display, J. Mol. Biol. 294 (1999) 163–180.
[27] J.D. Kotz, C.J. Bond, A.G. Cochran, Phage-display as a tool for quantifying protein stability determinants, Eur. J. Biochem. 271 (2004) 1623–1629.
[28] C.V. Lee, S.S. Sidhu, G. Fuh, Bivalent antibody phage display mimics natural immunoglobulin, J. Immunol. Methods 284 (2004) 119–132.
[29] Z. Han, C. Xiong, T. Mori, M.R. Boyd, Discovery of a stable dimeric mutant of cyanovirin-N (CV-N) from a T7 phage-displayed CV-N mutant library, Biochem. Biophys. Res. Commun. 292 (2002) 1036–1043.
[30] M. Widersten, B. Mannervik, Glutathione transferases with novel active sites isolated by phage display from a library of random mutants, J. Mol. Biol. 250 (1995) 115–122.